Comparison of Control Techniques & Modeling of 15-level cross H Bridge Multilevel Inverter

Suresh Kumar Tummala[1*], *Sameera* Shaik[1], *D Srinivasa* Rao[1], *Srinivas* Rao J[2], *Ibrahim H.* Al-Kharsan[3,4], *Dharmendra* Kumar[5]

[1] Gokaraju Rangaraju Institute of Engineering & Technology, Hyderabad, India
[2] Associate Professor, EEE Department, Anurag Engineering College, Kodad, TS, India-508206
[3] Computer Technical Engineering Department, College of Technical Engineering, The Islamic University, Najaf, Iraq
[4] Department of Electrical Engineering, Faculty of Engineering, University of Kufa, Najaf, 54001, Iraq
[5] Uttaranchal School of Computing Sciences, Uttaranchal University, Dehradun 248007 INDIA

Abstract This paper presents the simulation of a 15-level cross-H bridge multilevel inverter using control techniques like sinusoidal pulse width modulation and third harmonic injection pulse width modulation. This paper aims to enhance output voltage level using fewer switches and to decrease total harmonic distortion by improving overall efficiency. Compared to other inverter topologies cross H bridge topology uses a lesser number of switches and dc voltages. Analysis and simulation of 15-level cross H bridge MLI are performed and presented.
Keywords—Multilevel Inverter (MLI), Total Harmonic Distortion (THD), Sinusoidal Pulse Width Modulation (SPWM), Third Harmonic Injection Pulse Width Modulation (THI-PWM), Cross-Connected

Nomenclature

Abbreviation	Explanation
V_{ndc}	Number of DC voltage sources
V(t)	The output voltage of the multilevel inverter (MLI)
N_l	Number of levels
N_d	Number of switches in the current path respectively.
S_n	number of switches
a_0, a_n, b_n	These are the coefficients of the Fourier transform
θ_1	Conduction angle
f_m	Modulating wave's peak frequency

* Corresponding Author: sureshkumar255@gmail.com

F	Fundamental output frequency of the inverter
f_{cr}	Carrier wave's peak frequency,
V_m	Reference signal peak amplitude
V_{cr}	Carrier signal peak amplitude respectively, ma is the amplitude modulation index
V_{ref}	Reference voltage vector

1 Introduction

These days, MLI has acquired enormous consideration and has gotten more promoted in high/medium voltage and force applications with lower consonant substance and higher proficiency. MLI's are comprehensively utilized in energy area businesses for receptive force remuneration and drive control. The diverse customary geographies of staggered inverters are Neutral Point Clamped (NPC), Flying Capacitor (FC), and cascade H-Bridge inverters (CHB) [2-5]. In these natural features, cascade H bridge topology is broadly utilized due to its straightforward design, outrageous particularity, and no voltage balance issues. The principle disadvantage of this topology is the requirement for more force electronic segments with an increment in the quantity of levels which significantly expands cost, exchanging misfortunes, and diminishes the proficiency of the framework. To defeat these downsides, we are going with cross H bridge topology [1,10,11] which is more worthwhile over fell MLI as far as sounds in yield voltage and the quantity of switches. Along these lines, the expense is limited, and effectiveness is improved. The diverse control methods utilized in this paper are sinusoidal pulse width regulation (SPWM) [7,8] and third harmonic injection pulse width modulation (THI-PWM) [6,7]. Here, a 15-level inverter is examined principally and can be stretched out to quite a few levels.

2 Cross H bridge multilevel inverter topology

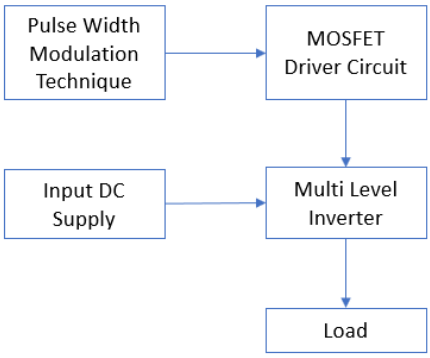

Fig. 1. Block diagram of 15-level cross H bridge multilevel inverter fed load

This topology consists of sixteen switches and seven DC voltage sources for a 1-ϕ, 15-level cross-H bridge inverter. Figure (1) shows a block diagram of a 15-level cross H bridge multilevel inverter [1,10,11] (MLI) fed with any load. In this paper, we have used resistive load and induction motor loads respectively. Figure (3) shows a single-phase 15-level cross H bridge inverter, whose switches and DC voltage sources are cross-connected and with suitable switching, the desired output voltage is generated. Figure (2) shows a three-phase

15-level cross H bridge inverter. The THD is improved using this topology compared to other topologies. Total fifteen output voltage levels $-7V_{dc}$, $-6V_{dc}$, $-5V_{dc}$, $-4V_{dc}$, $-3V_{dc}$, $-2V_{dc}$, $-V_{dc}$, 0, V_{dc}, $2V_{dc}$, $3V_{dc}$, $4V_{dc}$, $5V_{dc}$, $6V_{dc}$, $7V_{dc}$ are generated. Also, the odd-numbered switches operate in a complementary manner to the even-numbered switches. The switching pattern of the proposed topology is shown in Table (1) for figure (3).

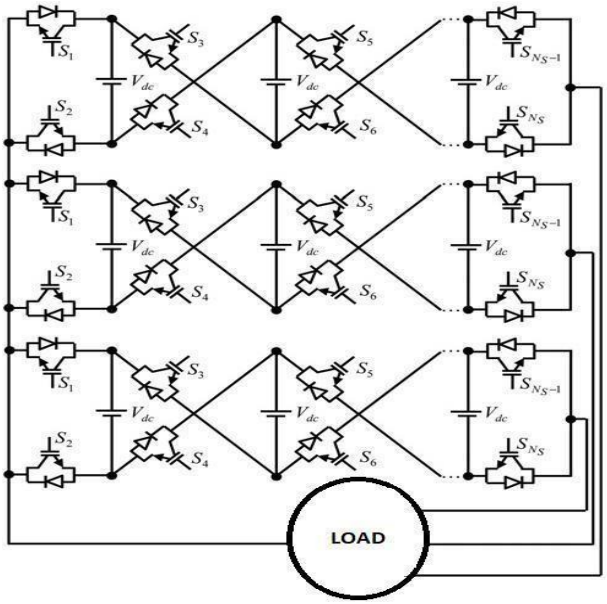

Fig. 2. Three-phase cross H bridge multilevel inverter (MLI)

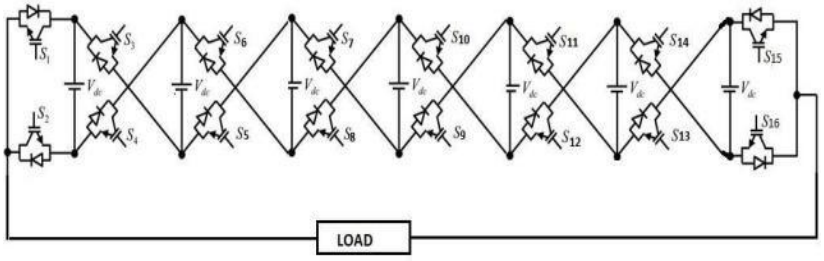

Fig. 3. Single-phase 15 level cross H bridge MLI [1]

The proposed topology is conventional and can be extended to any MLI by using the following formulae. In this topology, we have obtained generalized formulae for the number of levels and the total number of switches required is

$N_l = 2V_{ndc}+1$ (1)

$S_n = 2(V_{ndc}+1)$ (2)

From (1) & (2) equations we can write

$S_n = N_l+1$ (3)

Table 1: Switching sequence of 15- level cross H bridge MLI

S.No.	Output Voltage	ON Switches
1	0	$S_1S_3S_5S_7S_9S_{11}S_{13}S_{15}$
2	V_{dc}	$S_2S_3S_5S_7S_9S_{11}S_{13}S_{15}$
3	$2V_{dc}$	$S_2S_3S_6S_8S_{10}S_{12}S_{14}S_{16}$
4	$3V_{dc}$	$S_2S_3S_6S_7S_9S_{11}S_{13}S_{15}$
5	$4\ V_{dc}$	$S_2S_3S_6S_7S_{10}S_{12}S_{14}S_{16}$
6	$5\ V_{dc}$	$S_2S_3S_6S_7S_{10}S_{11}S_{13}S_{15}$
7	$6\ V_{dc}$	$S_2S_3S_6S_7S_{10}S_{11}S_{14}S_{16}$
8	$7\ V_{dc}$	$S_2S_3S_6S_7S_{10}S_{11}S_{14}S_{15}$
9	$-\ V_{dc}$	$S_1S_4S_6S_8S_{10}S_{12}S_{14}S_{16}$
10	$-2\ V_{dc}$	$S_1S_4S_5S_7S_9S_{11}S_{13}S_{15}$
11	$-3\ V_{dc}$	$S_1S_4S_5S_8S_{10}S_{12}S_{14}S_{16}$
12	$-4V_{dc}$	$S_1S_4S_5S_8S_9S_{11}S_{13}S_{15}$
13	$-5V_{dc}$	$S_1S_4S_5S_8S_9S_{12}S_{14}S_{16}$
14	$-6V_{dc}$	$S_1S_4S_5S_8S_9S_{12}S_{13}S_{15}$
15	$-7V_{dc}$	$S_1S_4S_5S_8S_9S_{12}S_{13}S_{16}$

3 Mathematical Formulae

The output voltage [1] of the multilevel inverter (MLI) can be computed from the Fourier series as shown below

$$V(t) = \frac{a_0}{2} + \sum_{n=1}^{\infty} (a_n \cos nwt + b_n \sin nwt) \quad (4)$$

Through the x-axis, there is the existence of quarter-wave symmetry. So, the coefficients a_0 and a_n become zero. Assume the symmetry across the y axis at ω = π /6, and $b_n$is defined as

$$b_n = \frac{1}{\pi}\left[\int_0^{\pi} (V_{dc}) \sin \omega t dwt\right] \quad (5)$$

After successive calculations the output voltage equation obtained as below

$$V(t) = \frac{4V}{\pi}\sum_{n=1}^{\infty} [\cos n\theta_1 + \cos n\theta_2 + \cos n\theta_3 + \cos n\theta_4 + \cos n\theta_5 + \cos n\theta_6 + \cos n\theta_7]\sin n\omega t \quad (6)$$

Exchanging points of MLI are accomplished by procuring nonlinear conditions from the specific harmonic elimination measure. From this technique, we can wipe out any chosen harmonic from the waveform. For 15 level, MLI with fifth, seventh, eleventh, thirteenth, seventeenth, and nineteenth harmonic disposal the accompanying conditions can be defined. The mathematical equations obtained to compute conduction angles are

$\cos\theta_1+\cos\theta_2+\cos\theta_3+\cos\theta_4+\cos\theta_5+\cos\theta_6+\cos\theta_7 = 7m$
$\cos5\theta_1+\cos5\theta_2+\cos5\theta_3+\cos5\theta_4+\cos5\theta_5+\cos5\theta_6+\cos5\theta_7 = 0$
$\cos7\theta_1+\cos7\theta_2+\cos7\theta_3+\cos7\theta_4+\cos7\theta_5+\cos7\theta_6+\cos7\theta_7 = 0$
$\cos11\theta_1+\cos11\theta_2+\cos11\theta_3+\cos11\theta_4+\cos11\theta_5+\cos11\theta_6+\cos11\theta_7 = 0$
$\cos13\theta_1+\cos13\theta_2+\cos13\theta_3+\cos13\theta_4+\cos13\theta_5+\cos13\theta_6+\cos13\theta_7 = 0$
$\cos17\theta_1+\cos17\theta_2+\cos17\theta_3+\cos17\theta_4+\cos17\theta_5+\cos17\theta_6+\cos17\theta_7 = 0$
$\cos19\theta_1+\cos19\theta_2+\cos19\theta_3+\cos19\theta_4+\cos19\theta_5+\cos19\theta_6+\cos19\theta_7 = 0$ (7)

From the above equation (7), the number seven indicates the magnitude of the Fourier series fundamental component which is at the right side of the first equation, and 'm' implies

modulation index. By iterating repeatedly with Newton Raphson (NR) [1] method conduction angles can be obtained. Those conduction angles are shown below

$$\theta_1 = 7.16, \theta_1 = 17.02, \theta_1 = 25.74, \theta_1 = 39.93, \\ \theta_1 = 52.36, \theta_1 = 58.28, \theta_1 = 67.30 \quad (8)$$

Also, the formula for total harmonic distortion (THD) is shown below

$$\%THD = \frac{\sqrt{\sum_{n=5,7,11,\dots}^{\infty} v_n^2}}{v_1} \times 1 \quad (9)$$

4 Sinusoidal pulse width modulation technique (SPWM)

The sinusoidal pulse width modulation technique [7,8] is a simple modulation technique used for harmonic reduction in inverters. In this technique, the pulse magnitude will be constant, and the pulse width is changed. Here, a reference wave is compared with a carrier wave and generates gate pulses. For this, a pure sine wave (reference) is compared with a triangular wave (carrier). The fundamental frequency is taken for the sine wave, and more than the fundamental frequency can be taken for the carrier wave. If the number of levels is N then (N-1) triangular carrier waves are required. So, a fifteen-level inverter requires fourteen carrier waves as shown in figure (4).

Two important parameters are defined in modulation techniques:

1. The frequency ratio $m_f = f_{cr}/f_m$
2. The amplitude modulation index is given below:

$m_a = V_m/(V_{cr}(m-1))$

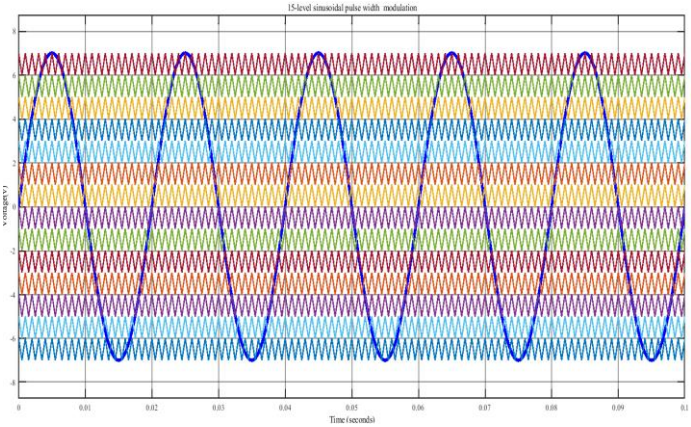

Fig. 4. Sinusoidal pulse width modulation for 15-level MLI

The fundamental frequency component in the inverter output voltage can be controlled by the amplitude modulation index. Where 'f_m' is the modulating wave's peak frequency, 'f_{cr}' is the carrier wave's peak frequency, 'V_m' is the reference signal peak amplitude and 'V_{cr}' is carrier signal peak amplitude respectively. The amplitude modulation index 'm_a' is usually adjusted by varying 'V_m' and keeping 'V_{cr}' fixed. The frequency of the reference signal determines inverter output frequency and its peak amplitude controls modulation index and in turn RMS output voltage. The SPWM scheme used here is level shifted in phase disposition (IPD) as it has a lower harmonic profile compared to other conventional techniques. Figure (4) shows level-shifted in-phase disposition sinusoidal pulse width modulation for a fifteen-level cross H-bridge inverter. The results can be seen in Table (3), and the fundamental three-phase output voltage can be seen in figure(7).

5 Third harmonic injection pulse width modulation technique (THI-PWM)

The sinusoidal pulse width modulation strategy is not difficult to carry out just as to comprehend. Yet, the principle downside of this technique is, it can't use the whole accessible DC bus supply voltage and subsequently this strategy approaches less of the greatest achievable output voltage. Along these lines, a third harmonic pulse width modulation technique [7] is acquainted with defeat this issue. In this technique, by adding a third harmonic signal in a low-frequency sinusoidal reference signal we can accomplish the abundancy expansion in output voltage waveform. The expansion of third harmonics implies that in one cycle of a sinusoidal wave, three patterns of harmonics will finish. The consequence of the addition of the third harmonic and fundamental harmonic is less in amplitude than the fundamental harmonic.

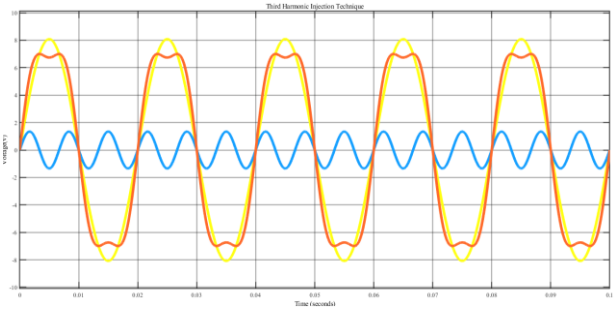

Fig. 5. Third harmonic injection technique

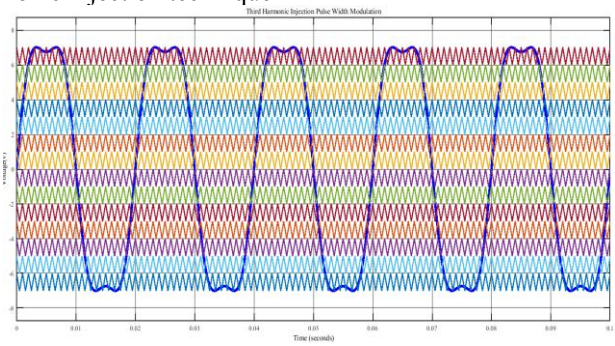

Fig. 6. Third harmonic injection pulse width modulation(THI-PWM)on 15-level cross H bridge inverter

This method helps the inverter in its performance enhancement. Figure (5) shows the third harmonic injection technique. In this paper, a basic third harmonic injection pulse width modulation is carried out for a fifteen-level inverter and the results can be seen in Table (3), and the fundamental output voltage can be seen in figure(13). Whereas figure (6) shows the third harmonic injection pulse width modulation (THI-PWM) on a 15-level cross H bridge inverter, where the third harmonic injected component with fourteen carrier waves are compared together to generate the gate pulses.

6 Simulation results

The simulations of cross H bridge multi-level inverter (MLI) are performed in MATLAB/SIMULINK domain. The schematic diagram of the presented topology can be

seen from figure (1). Switching sequences are shown in table (1). The parameters used for simulation are listed in table (2).

Table 2: Parameters used to carry out simulation

Parameters	Values
Line frequency	50Hz
Switching frequency	1000Hz
Load voltage	400v
DC voltage	10v

6.1 Simulation results for cross-bridge using sinusoidal pulse width modulation (SPWM)

Figures (7), (11) show fundamental three-phase output voltages for 15-level cross H bridge inverter and total harmonic distortion (THD) of R-Load.

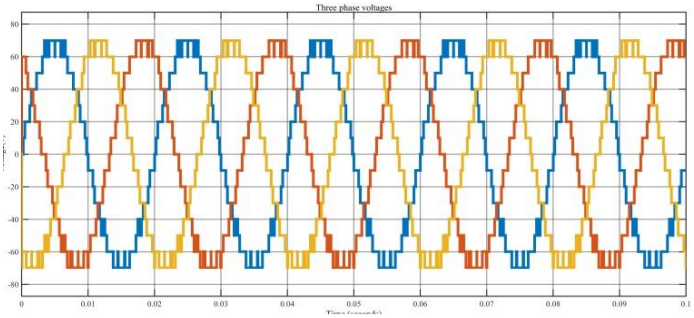

Fig. 7. Three-phase output voltages for 15-level cross H bridge using SPWM technique on R-load

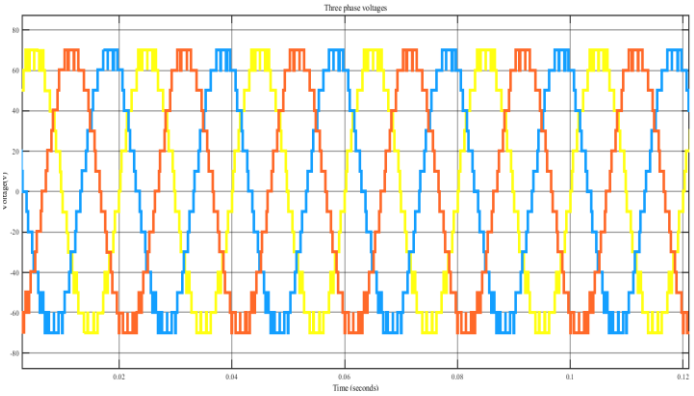

Fig. 8. Three-phase output voltages for 15-level cross H bridge using SPWM technique on induction motor load

Whereas figures (8), (9), (10), (12) shows fundamental three-phase output voltages, speed, torque characteristics, and lastly total harmonic distortion (THD) on induction motor load for 15-level cross H bridge inverter using sinusoidal pulse width modulation (SPWM) on induction motor load respectively.

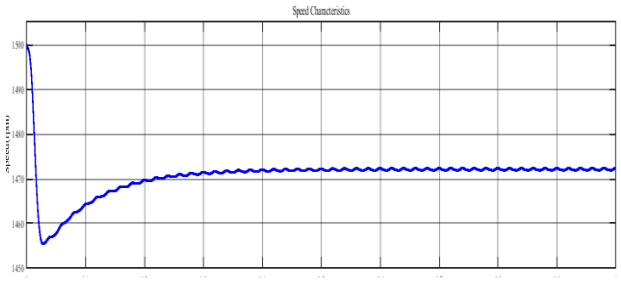

Fig. 9. Speed characteristics of induction motor using SPWM control technique

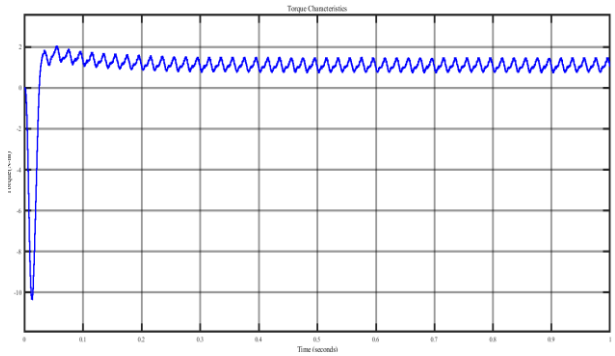

Fig. 10. Torque characteristics of induction motor using SPWM control technique

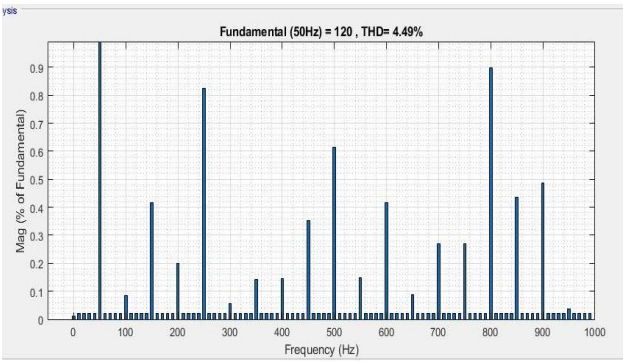

Fig. 11. Total harmonic distortion (THD) of SPWM on R-Load

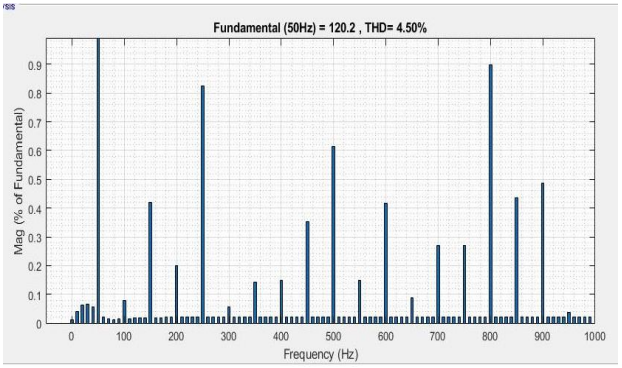

Fig. 12. Total harmonic distortion (THD) of SPWM on induction motor load

6.2 Simulation results for cross-bridge using third-harmonic injection pulse width modulation (THI-PWM)

Figures (13), (17) shows fundamental three-phase output voltages for 15-level cross H bridge inverter and total harmonic distortion (THD) of R-Load. Whereas figures (14), (15), (16), (18) shows fundamental three-phase output line voltages, speed, torque characteristics, and lastly total harmonic distortion (THD) on induction motor load for 15-level cross H bridge inverter using third-harmonic injection pulse width modulation (THI-PWM) on induction motor load respectively.

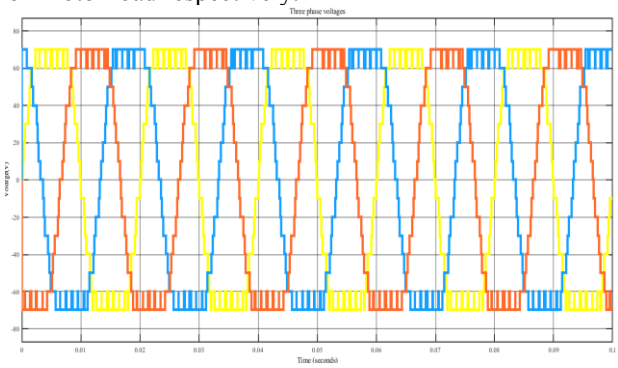

Fig. 13. Three-phase output voltages for 15-level cross H bridge using THI-PWM technique on R-load

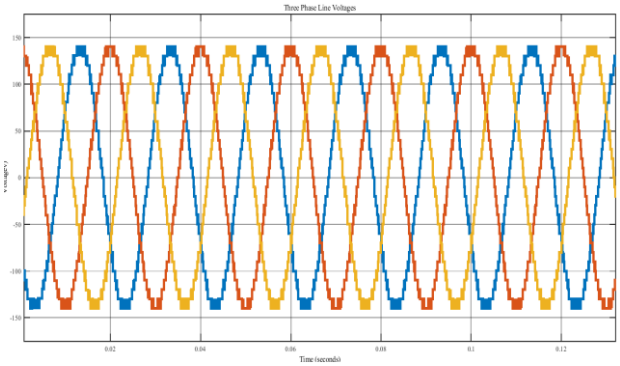

Fig. 14. Three-phase output line voltages for 15-level cross H bridge using SPWM technique on induction motor load

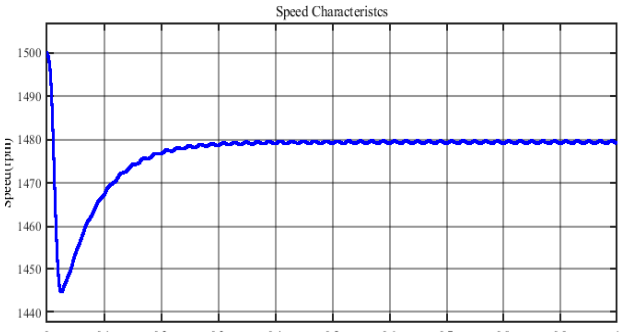

Fig.15. Speed characteristics of induction motor using THI-PWM control technique

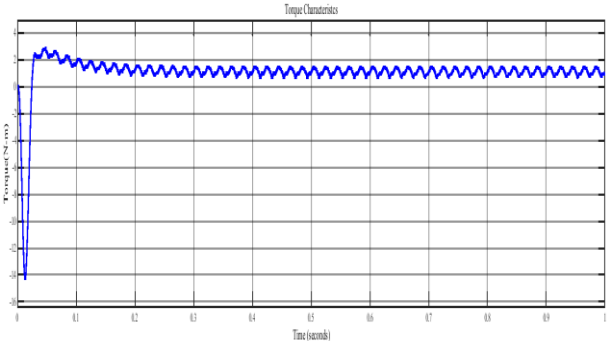

Fig. 16. Torque characteristics of induction motor using SPWM control technique

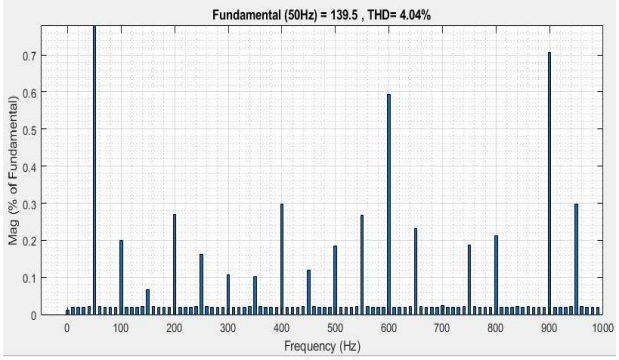

Fig. 17. Total harmonic distortion (THD) of THI-PWM on R-Load

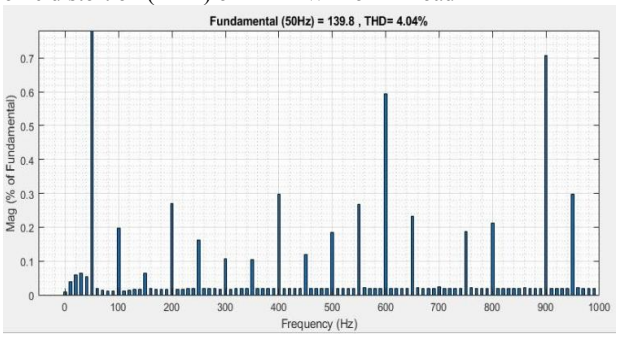

Fig. 18. Total harmonic distortion (THD) of THI-PWM on induction motor load

7 Comparison of SPWM and THI-PWM techniques

Here the obtained results from SPWM and THI-PWM techniques for 15-level cross H bridge topology are compared [10-15]. Four factors are taken into consideration for the comparison of induction motor load and two factors are considered for comparison of R-load. The factors that are considered for induction motor load are output fundamental L-L voltage magnitude, THD, speed, and torque characteristics respectively. The factors that are considered for R-load are output fundamental L-L voltage and THD respectively. Table (3) shows the comparison of different parameters for a 15-level cross H bridge using SPWM and THI-PWM. From table (3) we can conclude that the THI-PWM technique gives more output voltage, speed & torque, and fewer harmonic distortions compared to the SPWM technique. So, the THI-PWM technique is more desirable and preferred compared to the SPWM technique.

Table 3: Comparison of different parameters for 15-level cross H bridge using SPWM and THI-PWM techniques

Control method	Load	Voltage (L-L)	THD %	Speed(rpm)	Torque (N-M)
SPWM	Resistive	120V	4.5	-	-
SPWM	Induction Motor	120.2 V	4.5	1472	1.016
THI-PWM	Resistive	139.5 V	4.04	-	-
THI-PWM	Induction Motor	139.8 V	4.04	1479	1.043

8 Conclusion

In this paper control techniques like SPWM & THI-PWM are discussed and compared. From these techniques, we can conclude that THI-PWM is best suited compared to the SPWM technique in terms of voltage magnitude, THD, speed, and torque for induction motor load, whereas voltage magnitude and THD factors in the case of R-load. Also in this paper, we used a topology that uses less power electronic switches, the number of voltage sources compared to any other typical MLI topologies. Also, this cross-H bridge topology has low cost, switching losses, and high efficiency. 'N+1' switches are required for 'N' level inverter in cross H bridge topology.

Acknowledgement

Authors would like to thank All India Council for Technical Education (AICTE), Govt. of INDIA for sanction of grants under Research Promotion Scheme (RPS). *Grant Number: 8-174/RIFD/RPS(Policy-1)/2018-19 dt: 22 Nov 2019*.

References

1. B. Yogeswara Reddy, J. Srinivas Rao, T. Suresh Kumar, A. Nagarjuna, Int. Jol. of Inn. Tech. and Expl. Engg. 8, 11 (2019)
2. Patil Swapnil Sanjay, Patil Rupali Anaji, Patil S.K, *Symmetrical Multilevel Cascaded H Bridge Inverter Using Multicarrier SPWM Technique*, (2018).
3. B. Phani Teja, V. Srikanth Babu, T. Suresh Kumar, Int. Jol. of App. Engg. Research 10, 16 (2015).
4. C.Dhanamjayalu, S.Meikandasivam, (I-PACT, 2017).
5. S.Satish Kumar, M.sasikumar,(ICONSEM, 2016).
6. J. Srinivas Rao, P. Srinivasa Varma, T. Suresh Kumar, Int. Jol. of Power Electronics and Drive Systems 9, 3 (2018).
7. M. Kavitha, P. B. Bobba and D. Prasad, *Investigations and experimental study on Magnetic Resonant coupling based Wireless Power Transfer system for neighborhood EV's*, (IEEE ICPS 2016).
8. Basem Alamri, Saeed Alsharani, Mohamed Darwish, (UPEC, 2015).
9. Kavitha Merugu, Prasad Dinkar, Bobba Phaneendra Babu, IET Electric Power Appl.,

13, 8 (2019).
10. Mohammad Farhadi Kangarlu, Ebrahim Babaei, (IET Power Electro., 2013)
11. B. J. Varghese, P. B. Bobba and M. Kavitha, *Effects of coil misalignment in a four-coil implantable wireless power transfer system*, (IEEE PIICON 2016)
12. T.Tarezewski, L.M.Grzesiale (EPE, 2013)
13. Carlos Alberto, Lozano Espinosa, IEEE member, Ivonne Porocarrcro, and Mauricio Izquicrdo, (October 2012 IJWNS).
14. Kouro, S.Malinowski, M.Gopakumar.,(IEEE Trans.,Ind.Electron.,2010).
15. S.Thelemans, F.De Belie, and J.mclkebeek, *A Sensorless, PMSM Drive Using Test Signals Generated by a Multilevel Inverters*, (in the process) (ICEMS Conf., Nov.2009).